Real-Space Renormalization Yields Finite Correlations

Thomas Barthel,[1] Martin Kliesch,[1] and Jens Eisert[1,2]

[1]*Institute for Physics and Astronomy, Potsdam University, 14476 Potsdam, Germany*
[2]*Institute for Advanced Study Berlin, 14193 Berlin, Germany*

Real-space renormalization approaches for quantum lattice systems generate certain hierarchical classes of states that are subsumed by the multiscale entanglement renormalization Ansatz (MERA). It is shown that, with the exception of one spatial dimension, MERA states are actually states with finite correlations, i.e., projected entangled pair states (PEPS) with a bond dimension independent of the system size. Hence, real-space renormalization generates states which can be encoded with local effective degrees of freedom, and MERA states form an efficiently contractible class of PEPS that obey the area law for the entanglement entropy. It is further pointed out that there exist other efficiently contractible schemes violating the area law.

Renormalization group (RG) methods aim at solving many-body problems by treating energy scales in an iterative fashion, progressing from high to low energies [1]. One of its earliest formulations is the real-space RG which works by repeated steps of thinning out local degrees of freedom and rescaling of the system as in Kadanoff's block spin transformation [2]. In real-space RG approaches to quantum lattice models [3], in each RG step τ, the system is partitioned into small blocks. From those blocks high-energy states are eliminated and the Hamiltonian $\hat{H}_{\tau+1}$ for the renormalized system is obtained by applying the corresponding projection operators, exactly $\hat{H}_{\tau+1} = \hat{P}_{\tau+1} \hat{H}_\tau \hat{P}_{\tau+1}^\dagger$ or in some appropriate approximation, followed by a coarse graining of the lattice. This is iterated, e.g., until a step $\tau = T$ is reached where the renormalized system consists of a single small block for which the ground state $|gs_T\rangle$ can be obtained exactly. Applying the RG transformations in reverse order yields an approximation $\hat{P}_1^\dagger \hat{P}_2^\dagger \ldots \hat{P}_T^\dagger |gs_T\rangle$ to the ground state of the original model. Those states, generated by the real-space RG, fall into the class of so-called tree tensor networks (TTN) [4]. A recent more elaborate real-space RG scheme, the multiscale entanglement renormalization Ansatz (MERA) [5,6], a genuine simulation technique for strongly correlated systems, allows in each RG step for local unitary operations to be applied before the elimination of block basis states. The technique generates hence a more general class of states, referred to as MERA states; see Fig. 1.

Whereas the degrees of freedom of MERA and TTN states are organized in a hierarchical structure encoding correlations on different length scales, there exists a different class of so-called finitely correlated states where the degrees of freedom are organized in a strictly local manner. For $D = 1$ dimensional systems they are often referred to as matrix product states [7], and for $D \geq 1$ as tensor product Ansätze or projected entangled pair states (PEPS) [8]; Fig. 2. PEPS are the basis of powerful numeri-

cal techniques, such as the very successful density-matrix renormalization group [9].

In this Letter, we establish the surprising fact that, for $D > 1$, real-space RG, despite of the inherently hierarchical nature of the procedure, generates states that capture correlations by local degrees of freedom. More specifically, it is shown that MERA states form a subclass of PEPS, unifying both approaches. This also explains the failure of real-space RG for some situations for which merely anecdotal evidence had previously accumulated.

PEPS, TTN, and MERA are all tensor network states (TNS). In terms of an orthonormal product basis $|\boldsymbol{\sigma}\rangle = \bigotimes_{i=1}^N |\sigma_i\rangle$ for a lattice of N sites, TNS are of the form $\sum_{\boldsymbol{\sigma}} \psi_{\boldsymbol{\sigma}} |\boldsymbol{\sigma}\rangle$ where the expansion coefficients $\psi_{\boldsymbol{\sigma}}$ are encoded as a partially contracted set of tensors; Fig. 2. Recently, this notion has been generalized to the fermionic case [10]. For a PEPS, to each site i, a tensor A_i is assigned which has one physical index σ_i and further auxiliary indices—one for each nearest neighbor—which need to be contracted to obtain $\psi_{\boldsymbol{\sigma}}$; Fig. 2. For TTN and MERA,
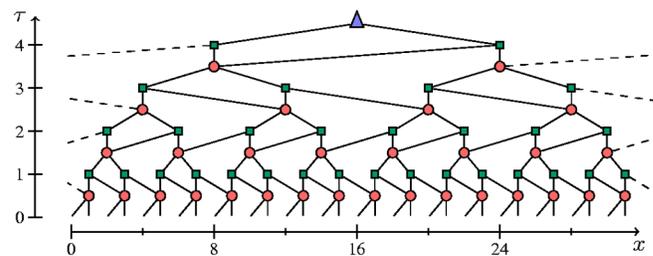
FIG. 1 (color online). A 1D MERA with linear branching ratio $b = 2$. Circles, squares, and the triangle denote tensors, the lines denote contractions of those tensors. The squares are isometries that map two local subsystems $\mathcal{H}_i^\tau$ and $\mathcal{H}_{i+1}^\tau$ into one $\mathcal{H}_{i/2}^{\tau+1}$ as in Kadanoff's block spin transformation. The circles denote unitary operators, disentanglers, reducing the entanglement between $\mathcal{H}_i^\tau \otimes \mathcal{H}_{i+1}^\tau$ and the rest of the system before the action of the isometry. Tensor positions are chosen according to Eq. (6) such that stacking of tensors is avoided.
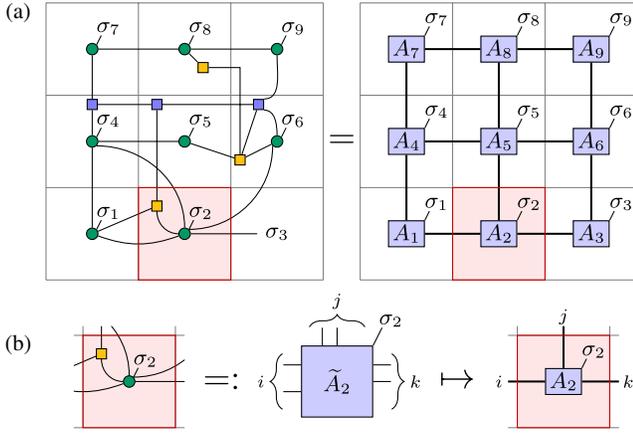
FIG. 2 (color online). (a) Procedure for mapping a TNS (left) to a 2D PEPS (right), by assigning tensors to lattice sites and contraction lines to paths on the lattice. (b) The elements of the PEPS tensors are determined by the elements of the tensors composing the TNS.

the tensors are arranged in a hierarchical pattern with the physical indices in the lowest layer; Fig. 1. The number of degrees of freedom of a TNS can be tuned by changing the number χ of values each auxiliary index runs over. Increasing χ for a fixed structure of the TNS enlarges the variational space, allowing for a more precise approximation to the exact ground state in a variational method, but increases computation costs. Hence, χ is called the refinement parameter of the TNS. The computational costs for efficient simulation techniques scale polynomially in χ.

For $D = 1$, TTN and MERA states can in general not be encoded efficiently as PEPS. There are MERA states with an entanglement entropy that scales logarithmically in the subsystem size [11], as occurring in critical models [12], whereas the entanglement entropy of 1D PEPS saturates for large subsystem sizes. In this respect, MERA states are more useful than PEPS for this case. For $D > 1$, however, our aforementioned result on real-space RG means in the tensor network language that MERA states with a refinement parameter χ can be mapped efficiently to PEPS such that the resulting PEPS refinement parameter χ_{PEPS} is some system-size independent function of χ. This also implies that $D > 1$ MERA states always obey the entanglement area law just as PEPS [12,13]. This behavior is shared by ground states of noncritical systems and critical bosons. Ground states of critical fermions, however, can violate the area law [12,14]. Consequently χ needs to be scaled polynomially in the system size in order to describe such critical fermionic systems accurately. Otherwise, the real-space RG schemes addressed here [3,5] are necessarily imprecise in that case. The remaining advantage of $D > 1$ MERA is that local observables and correlation functions can be evaluated efficiently, whereas, for PEPS, approximations are necessary. In this sense, MERA states simply form an efficiently contractible subclass of PEPS. This raises the question of whether any efficiently con-

tractible tensor network automatically yields an area law which is, however, not the case. To show this, we construct an example of efficiently contractible TNS based on unitary quantum cellular automata (QCA). For a specific choice of the tensors, one obtains instances that violate the area law for generic bipartitions of the system.

General procedure for mapping TNS to PEPS.—All TNS can be mapped to PEPS, although not necessarily in an efficient manner. To map a TNS to a PEPS one can (a) assign each tensor of the TNS to a specific site of the physical lattice [15]

$$\mathcal{V}_{\text{phys}} := \{0, \ldots, L - 1\}^D \subset \mathbb{Z}^D, \tag{1}$$

and (b) for each contraction line that connects the tensors, decide on a specific path for that line on the edges $\mathcal{E}_{\text{phys}}$ of the physical lattice,

$$\mathcal{E}_{\text{phys}} := \{(\boldsymbol{r}, \boldsymbol{r}') \in \mathcal{V}_{\text{phys}} \times \mathcal{V}_{\text{phys}} || \boldsymbol{r} - \boldsymbol{r}'|_1 = 1\}, \tag{2}$$

see Fig. 2. The tensors composing the PEPS are then obtained by introducing for each edge of the lattice an auxiliary vector space that is the tensor product of the vector spaces of all TNS contraction lines that traverse that edge. The elements of the PEPS tensor for site i are determined by the elements of all the TNS tensors that were assigned to site i. See Fig. 2(b).

Given a family of TNS for different linear system sizes L, a mapping of the TNS to PEPS is called efficient if there exists an upper bound χ_{PEPS} on the resulting PEPS refinement parameter that is independent of L. Applying the described mapping procedure for a 1D MERA state inevitably results in an inefficient mapping, i.e., in a PEPS refinement parameter χ_{PEPS} that diverges with the system size. This is not just a feature of the specific procedure. In [11], a family of 1D TTN states is constructed for which any mapping to PEPS necessarily requires χ_{PEPS} to diverge with the system size.

Qualitative argument.—The following argument motivates why an efficient mapping of MERA to PEPS should be possible for $D > 1$. Let us assign to each contraction line of the MERA state a finite cross section, e.g., equal to a^{D-1} with the lattice spacing a. Then one can ask what D-dimensional volume $V(\tau)$ the contraction lines of a certain layer τ connecting to layers with $\tau' \leq \tau$ cover. Those contraction lines of layer τ have length $\ell(\tau) \propto ab^{\tau}$, where b is the linear branching ratio of the MERA. The number of lattice cells in layer τ is $b^{(T-\tau)D}$; Fig. 1. Hence, the volume covered by the contraction lines of layer τ is $V(\tau) \propto a^{D-1}\ell(\tau)b^{(T-\tau)D} \propto b^{DT-(D-1)\tau}$. The density of the MERA contraction lines, or more precisely, a resulting estimate for the average number of contraction line paths traversing a unit cell of the physical lattice ($\tau = 0$) is hence

$$\log_\chi(\chi_{\text{PEPS}}) \propto b^{-TD} \sum_{\tau=0}^{T} V(\tau) \propto \sum_{\tau=0}^{T} b^{-(D-1)\tau}$$

$$\Rightarrow \log_\chi(\chi_{\text{PEPS}}) \propto \begin{cases} T & \text{for } D = 1 \\ \frac{1}{1-b^{-(D-1)}} & \text{for } D > 1, T \to \infty. \end{cases} \tag{3}$$

Note that for an edge traversed by n paths, one obtains an upper bound $\chi_{\text{PEPS}} = \chi^n$ to the PEPS refinement parameter, i.e., $n = \log_\chi(\chi_{\text{PEPS}})$. As $T = \log_b L$, 1D MERA with a fixed refinement parameter χ have according to Eq. (3) the potential to encode states with a logarithmic scaling of the entanglement entropy [11], as occurring in critical 1D systems. For $D > 1$, however, Eq. (3) suggests that there is enough space on the physical lattice to assign the MERA contraction lines to paths on the lattice such that the mapping to PEPS is efficient. That this is indeed possible is proven constructively in the following.

Preconditions for MERA states.—In order to show that the mapping presented in the following is efficient, it is necessary to exploit the defining properties of MERA states that correspond directly to features of the real-space RG and can be summarized as follows. (i) The MERA state is a TNS for a D-dimensional square lattice ($\mathcal{V}_{\text{phys}}, \mathcal{E}_{\text{phys}}$) consisting of L^D unit cells with

$$L = b^T. \tag{4}$$

(ii) The MERA consists of T layers of tensors labeled by $\tau = 1, \ldots, T$. (iii) There is an upper bound χ on the dimension of the vector spaces associated to the tensor indices, and an upper bound C_o on the order of each tensor. (iv) With each layer, we associate a coarse-grained square lattice $\mathcal{L}_\tau$ of $(L/b^\tau)^D$ cells of the physical lattice

$$\mathcal{L}_\tau := \{0, \ldots, L/b^\tau - 1\}^D \subset \mathbb{Z}^D, \tag{5}$$

and $\mathcal{L}_0 := \mathcal{V}_{\text{phys}}$. Every cell of lattice $\mathcal{L}_\tau$ contains corresponding b^D cells of lattice $\mathcal{L}_{\tau-1}$. (v) There exists an assignment of the tensors of layer τ to cells of the lattice $\mathcal{L}_\tau$ such that the number of tensors inside a single cell is bounded from above by a constant C_t, and the distance of contracted tensors is bounded from above by C_r, where the distance of a tensor of layer τ to a tensor of layer $\tau' \leq \tau$ is defined as the L_1 distance of their corresponding cells in $\mathcal{L}_\tau$ [16]. (vi) For $|\tau - \tau'| > C_T$, there are no contractions between tensors of layer τ with tensors of layer τ'.

The upper bounds χ, C_o, C_t, C_r, and C_T are required to be independent of the system size L. [17] The stated conditions guarantee that the MERA features a so-called causal cone [6]. Hence, local observables can be evaluated efficiently if all tensors are chosen isometric. As we require only upper bounds on the MERA refinement parameter, the apparent restriction to square lattices is not essential. The conditions stated above are met for all typical MERA structures considered in the literature so far. See Fig. 3(a) for a 2D MERA with $b = 2$, $C_o = 8$, $C_t = 2$, and $C_T = 1$, for which one can reach $C_r = 2$.

Efficiently mapping MERA to PEPS for $D > 1$.—Let us explain a general scheme for mapping MERA states for $D > 1$ dimensional systems efficiently to PEPS. The preconditions listed above are assumed to be given. A simple procedure to assign the MERA tensors to certain lattice sites is to put the tensors of cell $\boldsymbol{n} \in \mathcal{L}_\tau$ of layer τ to the site $\boldsymbol{r}_\tau(\boldsymbol{n}) = b^\tau \boldsymbol{n} \in \mathcal{V}_{\text{phys}}$. The problem with this ap-
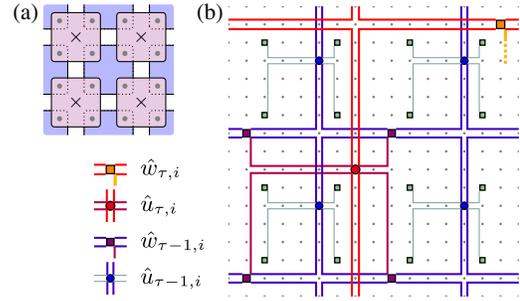
FIG. 3 (color online). (a) Unit cell of a specific 2D MERA state. With each layer, corresponding to a single RG step, unitary disentanglers are applied that reduce the entanglement between blocks of 2×2 sites with the rest of the system. Then, an isometry maps from those 2×2 sites (dots) into one (crosses). (b) Mapping of this MERA state to a PEPS. The diagram shows the assignment of two layers of the MERA, composed of disentanglers $\hat{u}$ and isometries $\hat{w}$, to the physical lattice.

proach is that one generates stacks of tensors at certain lattice sites, i.e., there exist positions $\boldsymbol{r} \in \mathcal{V}_{\text{phys}}$ to which a number of tensors is assigned that is not independent of the lattice size. For example, at site $\boldsymbol{r} = (0, \ldots, 0)$ a number of $\propto T = \log_b L$ tensors accumulate. Further stacks of tensors with height $\propto T'$ accumulate at lattice sites with coordinates $b^{T'}(1, \ldots, 1)$. It is necessary to avoid such stacks of tensors, because they imply in general that χ_{PEPS} diverges with the system-size. Stacks can be avoided by shifting the allowed tensor positions for different layers relative to each other. One possible such choice for $\boldsymbol{r}_\tau(\boldsymbol{n})$ is

$$\boldsymbol{r}_\tau(\boldsymbol{n}) = b^\tau \boldsymbol{n} + b^{\tau-1} \boldsymbol{e} \in \mathcal{V}_{\text{phys}} \quad \text{with} \quad \boldsymbol{n} \in \mathcal{L}_\tau \tag{6}$$

and $\boldsymbol{e} := (1, \ldots, 1) \in \mathbb{Z}^D$ as demonstrated in Fig. 1. With this choice, two tensors can end up at the same site only if they belong to the same layer $\mathcal{L}_\tau$ and the same lattice cell $\boldsymbol{n}$ within that layer. The possible tensor positions of layers τ form disjoint sublattices $\mathcal{V}_\tau$ of the physical lattice.

$$\mathcal{V}_\tau := \{\boldsymbol{r}_\tau(\boldsymbol{n}) | \boldsymbol{n} \in \mathcal{L}_\tau\} \subset \mathcal{V}_{\text{phys}}, \quad \mathcal{V}_\tau \cap \mathcal{V}_{\tau' \neq \tau} = \varnothing.$$

All coordinates r_i of $\boldsymbol{r} \in \mathcal{V}_\tau$ have a b-adic valuation of $\tau - 1$, where the b-adic valuation $v_b(n)$ of an integer n is defined such that $v_b(n) = \tau$ iff τ is the largest integer such that $n \bmod b^\tau = 0$, for example, $v_2(12) = 2$. Avoiding stacks of tensors is not sufficient for an efficient PEPS encoding. In $D = 1$, all contraction lines are assigned to paths that necessarily stack up on the x axis, Fig. 1. This stacking of the paths can be avoided in $D > 1$ by assigning contraction lines between tensors of layers τ and τ' to paths that are restricted to edges from subgrids $\mathcal{E}_\tau$ and $\mathcal{E}_{\tau'}$ and that are shortest paths with respect to the L_1 distance on $\mathcal{V}_\tau \cup \mathcal{V}_{\tau'}$. Here, a grid $\mathcal{E}_\tau$ is defined as the subset of physical edges connecting nearest neighbors of the lattice $\mathcal{V}_\tau$ on straight lines; see Fig. 4.

$$\mathcal{E}_\tau := \{(\boldsymbol{r}, \boldsymbol{r} + \boldsymbol{e}_i) \in \mathcal{E}_{\text{Phys}} | v_b(r_j) = \tau - 1 \; \forall \; j \neq i\}$$
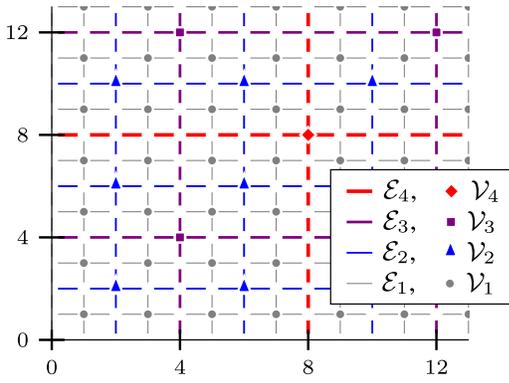
FIG. 4 (color online). Disjoint sublattices $\mathcal{V}_\tau \subset \mathcal{V}_{\text{phys}}$ to which MERA tensors are assigned and disjoint subsets of edges $\mathcal{E}_\tau \subset \mathcal{E}_{\text{phys}}$ to which MERA contraction lines are assigned for $b = 2$. In our construction, the paths assigned to contraction lines from tensors of layer 2 to tensors in layer 3 are, e.g., restricted to edges from $\mathcal{E}_2 \cup \mathcal{E}_3$.

with $[e_i]_j = \delta_{i,j}$. Hence $\mathcal{E}_\tau \cap \mathcal{E}_{\tau'} = \varnothing \, \forall_{\tau \neq \tau'}$. For this choice of tensor positions and paths of MERA contraction lines an upper bound for the resulting PEPS refinement parameter χ_{PEPS} follows: Contraction lines assigned to an edge $e = (\bm{r}, \bm{r}') \in \mathcal{E}_\tau$ contract tensors of layer τ with tensors of layers τ' where $|\tau' - \tau| \leq C_T$. For a layer τ' with $\tau' > \tau$, tensors from at most $(2C_r)^D$ cells of $\mathcal{L}_{\tau'}$ around the cell corresponding to site $\bm{r}$ can have contraction line paths traversing edge e. From the layers τ' with $\tau' \leq \tau$, tensors of at most $(2C_r)^D \sum_{t=0}^{C_T} b^{Dt}$ cells can contribute. Thus, the number of contraction line paths traversing edge e and hence $\log_\chi(\chi_{\text{PEPS}})$ are bounded from above by

$$\log_\chi(\chi_{\text{PEPS}}) \leq (2C_r)^D (C_T + b^{D(C_T+1)}) C_t C_o. \quad (7)$$

As this upper bound is independent of the system size, the presented mapping of MERA to PEPS is efficient.

The scheme displayed in Fig. 3(b) for mapping the 2D MERA defined in Fig. 3(a) to a PEPS results in the PEPS refinement parameter $\chi_{\text{PEPS}} = \chi^6$. In the supplement [11], the notion of a refined PEPS is introduced which allows for a favorable scaling, $\chi_{\text{PEPS}}^{\text{refined}} = \chi^2$ in this case.

QCA violating the area law.—Let us point out that, also for $D > 1$, there exist efficiently contractible TNS that violate the entanglement area law; more details in [11]. Consider a QCA consisting of $2T$ layers, where in every layer, $(L/2)^D$ local unitary gates are applied to plaquettes of $2 \times \ldots \times 2$ sites each. For $T = (\log L)^{1/D}$, the computation cost for the evaluation of local observables with respect to such QCA is polynomial in L, namely $O(L^2 (\log L)^{1/D})$. At the same time, one finds for a suitable choice of the unitary gates and generic choices for subsystems $\mathcal{A}_L$ with $\text{Vol}\mathcal{A}_L \propto L^D$ an entanglement entropy of $S_{\mathcal{A}_L} = \Omega(L^{D-1}(\log L)^{1/D})$ which violates the area law.

Conclusion.—In this Letter, we have shown that MERA states for $D > 1$ can be efficiently encoded as PEPS. From a physical perspective, the result implies that real-space

RG techniques, despite the scale-invariant features of the TNS they generate, give rise to states that can be encoded with local degrees of freedom. As a corollary, it follows that $D > 1$ MERA states obey the area law for the entanglement entropy [12,13]. Consequently, the refinement parameter χ needs to be scaled polynomially in the system size in order to describe $D > 1$ critical fermionic systems accurately. Otherwise, the real-space RG schemes addressed here [3,5] are imprecise for such systems.

[1] K. G. Wilson, Rev. Mod. Phys. **47**, 773 (1975); F. J. Wegner, Phys. Rev. B **5**, 4529 (1972).
[2] L. Kadanoff, Physics **2**, 263 (1966).
[3] R. Jullien, J. Fields, and S. Doniach, Phys. Rev. Lett. **38**, 1500 (1977); S. D. Drell, M. Weinstein, and S. Yankielowicz, Phys. Rev. D **16**, 1769 (1977).
[4] Y.-Y. Shi, L.-M. Duan, and G. Vidal, Phys. Rev. A **74**, 022320 (2006).
[5] G. Vidal, Phys. Rev. Lett. **99**, 220405 (2007).
[6] G. Vidal, Phys. Rev. Lett. **101**, 110501 (2008).
[7] M. Fannes, B. Nachtergaele, and R. F. Werner, Commun. Math. Phys. **144**, 443 (1992); S. Rommer and S. Östlund, Phys. Rev. B **55**, 2164 (1997).
[8] H. Niggemann, A. Klümper, and J. Zittartz, Z. Phys. B **104**, 103 (1997); T. Nishino, K. Okunishi, Y. Hieida, N. Maeshima, and Y. Akutsu, Nucl. Phys. B **575**, 504 (2000); M. A. Martín-Delgado, M. Roncaglia, and G. Sierra, Phys. Rev. B **64**, 075117 (2001); F. Verstraete and J. I. Cirac, arXiv:cond-mat/0407066.
[9] S. R. White, Phys. Rev. Lett. **69**, 2863 (1992); U. Schollwöck, Rev. Mod. Phys. **77**, 259 (2005).
[10] C. V. Kraus, N. Schuch, F. Verstraete, and J. I. Cirac, arXiv:0904.4667; P. Corboz, G. Evenbly, F. Verstraete, and G. Vidal, Phys. Rev. A **81**, 010303(R) (2010); C. Pineda, T. Barthel, and J. Eisert, Phys. Rev. A **81**, 050303 (R) (2010); T. Barthel, C. Pineda, and J. Eisert, Phys. Rev. A **80**, 042333 (2009).
[11] See supplementary material at http://link.aps.org/supplemental/10.1103/PhysRevLett.105.010502 for a mapping to refined PEPS and for TNS that exceed the area law.
[12] L. Amico, R. Fazio, A. Osterloh, and V. Vedral, Rev. Mod. Phys. **80**, 517 (2008); J. Eisert, M. Cramer, and M. B. Plenio, Rev. Mod. Phys. **82**, 277 (2010).
[13] G. Vidal, arXiv:quant-ph/0610099v1.
[14] M. M. Wolf, Phys. Rev. Lett. **96**, 010404 (2006); D. Gioev and I. Klich, Phys. Rev. Lett. **96**, 100503 (2006); T. Barthel, M.-C. Chung, and U. Schollwöck, Phys. Rev. A **74**, 022329 (2006); W. Li et al., Phys. Rev. B **74**, 073103 (2006); M. Cramer, J. Eisert, and M. B. Plenio, Phys. Rev. Lett. **98**, 220603 (2007).
[15] For clarity we restrict to square lattices.
[16] The coarse-graining maps cells from $\mathcal{L}_{\tau'}$ to cells in $\mathcal{L}_{\tau > \tau'}$.
[17] Actually, a system-size independent upper bound on the combination occurring in Eq. (7) is sufficient.